SYNTHESIS AND CHARACTERIZATION OF ZnO NANOSTRUCTURES AND SYNTHESIS OF Zn/Al_2O_3 NANOCOMPOSITE BY MECHANICAL ALLOYING ROUTE

A THESIS SUBMITTED IN PARTIAL FULFILMENT OF THE

REQUIREMENTS FOR THE DEGREE OF

Master of Technology
In
Metallurgical and Materials Engineering

Submitted by

Madhukar Poloju

Roll No. 209MM1239

Department of Metallurgical & Materials Engineering
National Institute of Technology
Rourkela

2010-2011

SYNTHESIS AND CHARACTERIZATION OF ZnO NANOSTRUCTURES AND SYNTHESIS OF Zn/Al_2O_3 NANOCOMPOSITE BY MECHANICAL ALLOYING ROUTE

A THESIS SUBMITTED IN PARTIAL FULFILMENT OF THE

REQUIREMENTS FOR THE DEGREE OF

Master of Technology
In
Metallurgical and Materials Engineering

Submitted by

Madhukar Poloju

Roll No. 209MM1239

Under the supervision of

Dr. S. N. Alam

Department of Metallurgical & Materials Engineering
National Institute of Technology
Rourkela

2010-2011

CERTIFICATE

This is to certify that Mr. MADHUKAR POLOJU, Reg No. 209MM1239 has carried out his project on the topic entitled "**Synthesis and Characterization of ZnO Nanostructures and Synthesis of Zn/Al_2O_3 Nanocomposite by Mechanical Alloying Route"** under my supervision and this part of the work has not been presented earlier in Department of Metallurgy and Material Engineering, NIT-Rourkela.

Date:

Dr. S. N. ALAM

Dept. of Metallurgical and Material Engineering,

National Institute of Technology

Rourkela-769008

Acknowledgement

I express my sincere gratitude to **Dr. S. N. ALAM**, Assistant Professor of the Department of Metallurgical and Material Engineering, National Institute of Technology, Rourkela, for giving me this great opportunity to work under his guidance. I am also thankful to him for his valuable suggestions and constructive criticism which has helped me in the development of this work. I am also thankful to his optimistic nature which has helped this project to come a long way through.

I am sincerely thankful to Dr B. B. Verma, Professor and Head of Metallurgical and Materials Engineering Department for providing me necessary facility for my work. I express my sincere thanks to Prof. B. C. Ray and Prof M. Kumar, the M.Tech Project co-ordinators of Metallurgical & Materials Engineering department.

Special thanks to my family members always encouraging me to higher studies, all department members specially Mr. Rajesh, Lab assistant of SEM lab and Mr. Sahoo, Lab assistant of Material Science lab all my friends of department of Metallurgical and Materials Engineering for being so supportive and helpful in every possible way.

MADHUKAR POLOJU

Roll No. : 209MM1239

LIST OF FIGURES

LIST OF TABLES

Abstract

We report simple methods to synthesize Zinc oxide nanostructures, without using catalysis with less complicity. This was done by oxidation of zinc foil at various temperatures (200^oC-1000^oC) and various times (1-3h) and also we find that the nanostructures size and shape depends on heating rate, temperature and heating time. Apart from oxidation of zinc we also find zinc oxide nanostructures in Zn-C dry battery. This nanostructure is formed on inner surface of Zn container (which acts as anode). These nanostructures are formed due reaction between electrolyte (mixture composed of manganese (IV) dioxide (MnO_2), ammonium chloride (NH_4Cl) and zinc chloride ($ZnCl_2$)) and Zn container. In Zn–C cell we find hierarchical and rod like structures. From oxidation of Zn we find rod and leaf like nanostructures. These oxide structures were characterized by SEM, EDX, XRD and DSC. We also synthesized the Zn/Al_2O_3 metal matrix composite by mechanical alloying method, in this we use oxidized Zn at 800^oC for 2h and Al powder in the stoichiometric ratio. The ZnO and Al is milled in planetary ball milling for 30h. During milling displacement reaction takes place and forms Zn/Al_2O_3 nanocomposite. This nanocomposite is characterized by XRD, SEM, EDX and DSC.

CONTENTS

CHAPTER 1

INTRODUCTION

1. INTRODUCTION:

Materials of nanostructure have received much attention of research because of their novel properties, which differ from those of bulk materials. ZnO is one of the few dominant nanomaterials for nanotechnology and zinc oxide belongs probably to the biggest group of one dimensional nanostructures. Zinc oxide (ZnO) has a wide direct band gap (3.37 eV) and a relative large excitation binding energy (60 meV) compared to thermal energy (26meV) [1]. A wide band gap has many benefits like enabling high temperature and power operations, reducing electronic noise, making sustenance in large electric fields possible and raising breakdown voltages. By proper alloying with MgO or CdO, the band gap can be tuned in the range of 3-4 eV. ZnO is also called as II–VI semiconductor, because Zn belongs to II group, and O_2 belongs to VI group in the periodic table. ZnO exhibits the most splendid and abundant configurations of nanostructures that one material can form. Owing to its unique properties and potential application in solar cell, electro and photo-luminescence devices, chemical sensors and so on, ZnO becomes an attractive inorganic material. ZnO with hierarchical structure has fundamental importance to understand the growth habit of ZnO crystal; moreover, considering their high surface to volume ratio, they are of great physical or chemical activities in gas-sensor and photo-catalysis. Zinc oxide (ZnO) received much attention because of its unique piezoelectric properties made suitable for surface acoustic wave devices, optical fibers and up to electronic devices. Due to the high optical band gap [2, 3]. ZnO films have been used as window layers in copper indium diselenide based hetero junction solar cells to enhance the short circuit current [4]. Another important advantage of ZnO is its chemical stability in the presence of hydrogen plasma which enable for use in the amorphous silicon solar cell fabrication by plasma enhanced chemical vapor deposition.

The study of one-dimensional nanostructural ZnO has attracted much interest owing to its low cost; it's unique electrical, optoelectronic, and luminescent properties; and its many potential applications in devices, such as solar cells, luminescent devices, and chemical detectors [4]. ZnO nanostructures have many potential applications in various fields. ZnO is used in biomedical applications, high temperature solid lubricant in gas turbine engines and electro chromic devices. Depending on ZnO nanostructure and shape there many applications. The shape of the

nanostructure depends on synthesis parameters. The various shapes of ZnO nanostructures are nanorings, nanobelts, nanotapes, nanorods, nanowires, etc.. Among these nanorods are used for gas sensing applications.

There are many methods to synthesize ZnO nanostructures such as chemical vapor deposition [5], physical vapor deposition [6] and molecular beam epitaxy [7]. ZnO nanowires have been synthesized simply by heating Zn powders containing catalyst nanoparticles [8], optically pumped nanowires [9]. The vapor–liquid–solid (VLS) mechanism is responsible for the nano-wire growth, in which a metal or an oxide catalyst is necessary to dissolve feeding source atoms in a molten state initiating the growth of nano-materials. However, most of the methods create ZnO nanostructures by using a catalyst, but there are some methods to form ZnO nanostructures without using catalyst, one of such method is ZnO nanorods formation by Zn oxidation is simple method and without complexity. The oxidation method is most attractive method because from this method we can synthesize different type of nanostructure [10, 11].

Among the composites Aluminum-based composite has been widely used in many fields owing to its excellent properties. Mainly Aluminum-based metal matrix composites (MMCs) are ideal materials for structural applications in the aerospace and automotive industries due to their high strength-to-weight ratio [12, 13]. Traditionally, particulate metal matrix composites are produced by adding reinforcement particles to the metal matrix in liquid state [14]. Many methods were studied to prepare aluminum-based composites. In the liquid methods, particles are added to liquid aluminium by stirring before casting. For this method exact uniform distribution is not possible especially in nano scale it is very difficult to get uniform distribution. To get uniform distribution in nano scale some new techniques are used like ultrasonic stirring of the metal melt [15, 16], high-energy mechanical milling [17, 18] and internal oxidation [19, 20]. Liquid state synthesis of metal matrix composite is difficult due to the difference in thermal expansion coefficients between ceramic particles and molten Al constituents and the poor wetability between these two become an obstacle to the liquid method used for synthesizing Al matrix composite [14]. To overcome this problem by introducing the solid state alloying, in this method we get uniform distribution.

We use mechanical alloying technique to synthesize the Zn/Al_2O_3 metal matrix composite, for this we use oxidized Zn foil (oxidized at 800^oC for 2h) and Al powder. This is a solid-state powder processing technique involving repeated deformation, welding and fracturing of powder particle. A displacement reaction takes place during ball milling of Al with Zinc oxide according to the following reaction [21, 22]

$$3MO + 2Al \rightarrow Al_2O_3 + 3M$$

CHAPTER 2

LITERATURE SURVEY

2.1 Properties of ZnO:

2.1.1 Crystal structure of ZnO

2.1.2 Mechanical properties

2.1.3 Electronic properties

2.1.4 Optical Properties

2.1.5 In below table we mention some physics properties of ZnO

2.2 Synthesisc techniques

2.2.1 Physical vapor deposition (PVD)

2.2.2 Chemical vapor deposition (CVD

2. LITERATURE REVIEW:

2.1 Properties of ZnO:

2.1.1 Crystal Structure of ZnO: [44]

Zinc oxide crystallizes in three forms: hexagonal wurtzite, cubic zincblende, and the rarely observed cubic rocksalt. The wurtzite structure is most stable at ambient conditions and thus most common. The zincblende form can be stabilized by growing ZnO on substrates with cubic lattice structure. In both cases, the zinc and oxide centers are tetrahedral. The rocksalt (NaCl-type) structure is only observed at relatively high pressures about 10 GPa.

Hexagonal and zincblende polymorphs have no inversion symmetry (reflection of a crystal relatively any given point does not transform it into itself). This and other lattice symmetry properties result in piezoelectricity of the hexagonal and zincblende ZnO, and in pyroelectricity of hexagonal ZnO.

More stable state of ZnO is wurtzite structure, which has a hexagonal unit cell with lattice parameters a = 0.3296, and c = 0.52065 nm. The oxygen anions and Zn cations form a tetrahedral unit. The entire structure lacks of central symmetry. The structure of ZnO can be simply described as a number of alternating planes composed of tetrahedrally coordinated O^{2-} and Zn^{2+} ions, stacked alternatively along the c-axis [23-27]. This is shown in the figure 2.1

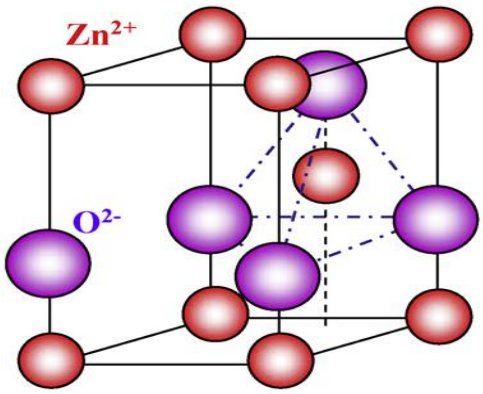

Figure 2.1 Crystal structure of the ZnO (the of tetrahedrally coordinated O^{2-} and Zn^{2+} ions).

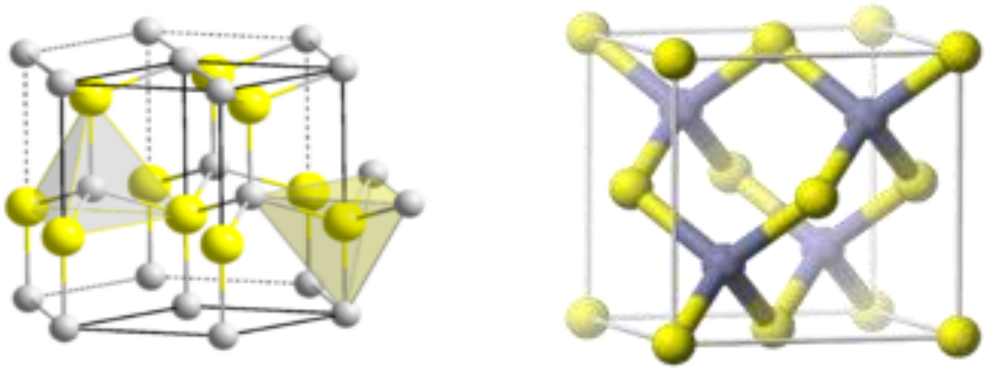

Figure 2.2 Wurtzite structure model of ZnO, which has non-central symmetry [23].

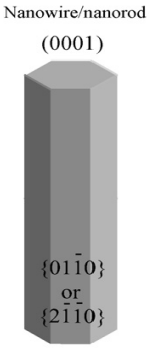

Figure 2.3 The ZnO Nano rod structure is shown below figure. It was grow vertically to the ZnO foil [23].

2.1.2 Mechanical Properties:

ZnO is a relatively soft material with approximate hardness of 4.5 on the Mohs scale. Its elastic constants are smaller than those of relevant III-V semiconductors, such as GaN. The high heat capacity and heat conductivity, low thermal expansion and high melting temperature of ZnO are beneficial for ceramics Among the tetrahedrally bonded semiconductors, it has been stated that ZnO has the highest piezoelectric tensor or at least one comparable to that of GaN and AlN. This property makes it a technologically important material for many piezoelectrical applications, which require a large electromechanical coupling.

The Al–13.8 wt%Zn/5 vol%Al_2O_3 bulk nanocomposite can be synthesized by Al–ZnO powder mixture after 60h milling and hot pressing at 500◦C under 400MPa pressure. The relative density of the hot pressed samples increased (from 95% to 99.6%) as the temperature increased (from 400 to 500◦C). Al crystallite size for both samples remained constant after annealing at

500 ◦C for 20 min. The hardness value for Al–13.8 wt.% Zn/5 vol%Al_2O_3 nanocomposite (relative density about 99.6% and crystallite size about 40 nm) was about 180HV and for Al–13.8 wt. % Zn (relative density 99.8% and crystallite size of about 40 nm) was about 150 HV [28].

2.1.3 Electronic Properties:

ZnO has a relatively large direct band gap of ~3.3 eV and a relatively large excitation binding energy (60 meV) compared to thermal energy (26meV) at room temperature. Advantages associated with a large band gap include higher breakdown voltages, ability to sustain large electric fields, lower electronic noise, and high-temperature and high-power operation. The bandgap of ZnO can further be tuned to ~ 3-4 eV by its alloying with magnesium oxide or cadmium oxide.

Most ZnO has n-type character, even in the absence of intentional doping. Reliable p-type doping of ZnO remains difficult. This problem originates from low solubility of p-type dopants and their compensation by abundant n-type impurities. Current limitations to p-doping do not limit electronic and optoelectronic applications of ZnO, which usually require junctions of n-type and p-type material. Known p-type dopants include group-I elements Li, Na, K; group-V elements N, P and As; as well as copper and silver. However, many of these form deep acceptors and do not produce significant p-type conduction at room temperature.

2.1.4 Optical Properties:

ZnO nanostructure material has good optical properties. ZnO nanostructures have very wide range of applications in optical filed. ZnO nanorods are very useful in laser to very fast optical pumping, to make population inversion in energy levels. And produce high power laser beams. ZnO is a wide band gap semiconductor that displays luminescent properties in the near ultra violet and the visible regions. The emission properties of ZnO nanoparticles in the visible region widely depend on their synthetic method as they are attributable to surface defects.

The Photoluminescence (PL) spectra of ZnO nanostructures have been widely reported. Excitonic emissions have been observed from the PL spectra of ZnO nanorods. It is shown that if we confine the quantum size then it can greatly enhance the exciton binding energy but an

interesting observation is that the green emission intensity increases with a decrease in the diameter of the nanowires. This is because of the larger surface-to-volume ratio of thinner nanowires which favours a higher level of defects and surface recombination. Red luminescence band has also been reported for which doubly ionized oxygen vacancies are considered responsible. Quantum confinement was also observed to be responsible in causing a blue shift in the near UV emission peak in the ZnO nanobelts. Some other fields of application include optical fibers, surface acoustic wave devices, solar cells etc [29, 30].

2.1.5 Physical Properties of ZnO [31, 32]:

Property	Value
Molecular formula	ZnO
Molar mass	81.4084 g/mol
Appearance	Amorphous white or yellowish white powder.
Odour	Odourless
Density	5.606 g/cm^3
Melting point	1975 °C
Boiling point	2360 °C
Solubility in water	0.16 mg/100 mL
Refractive index	2.0041
Lattice Constants	a_o = 0.32469 Å c_o = 0.52069Å
Relative Dielectric Constant	8.66
Energy Gap	3.4 eV Direct
Intrinsic Carrier Concentration	< 10^6 /cc
Exciton Binding Energy	60 meV
Electron effective mass	0.24
Electron mobility (at 300 K)	200 cm^2/V.sec.
Hole Effective mass	0.59
Hole mobility (at 300 K)	5-50 cm^2/V.sec

2.2 Synthesis Techniques: [44]

We have lot of techniques to synthesize ZnO nanostructures. These techniques are mainly divided into 3 categories that are shown below table.

SYNTHESISE TECHNIQUES	SUB CATEGORIES
Physical vapour deposition (**PVD**)	Cathodic Arc Deposition Electron beam physical vapor deposition Evaporative deposition Pulsed laser deposition Sputter deposition
Chemical vapour deposition (CVD)	Vapour phase epitaxy (VPE) Rapid thermal CVD (RTCVD) Hybrid Physical-Chemical Vapour Deposition (HPCVD) Metalorganic chemical vapour deposition (MOCVD) Hot wire CVD (HWCVD) Atomic layer CVD (ALCVD) Plasma-Enhanced CVD (PECVD)
CHEMICAL	In this nanostructures synthesis by chemical reaction

2.2.1 Physical Vapour Deposition (PVD):

Physical vapor deposition (PVD) is a variety of vacuum deposition and is a general term used to describe any of a variety of methods to deposit thin films by the condensation of a vaporized form of the material onto various surfaces (e.g., onto semiconductor wafers). The coating method involves purely physical processes such as high temperature vacuum evaporation. PVD have different subcategories that are shown below.

Cathodic Arc Deposition: In which a high power arc discharged at the target material blasts away some into highly ionized vapor.

Electron Beam Physical Vapor Deposition: In which the material to be deposited is heated to a high vapor pressure by electron bombardment in "high" vacuum.

Evaporative Deposition: In which the material to be deposited is heated to a high vapor pressure by electrically resistive heating in "low" vacuum.

Pulsed Laser Deposition: In which a high power laser ablates material from the target into a vapor [44].

Sputter Deposition: In which a glow plasma discharge (usually localized around the "target" by a magnet) bombards the material sputtering some away as a vapor.

2.2.2 Chemical Vapor Deposition (CVD) [35]:

Chemical vapor deposition (CVD) is a chemical process used to produce high-purity, high-performance solid materials. The process is often used in the semiconductor industry to produce thin films. In a typical CVD process, the wafer (substrate) is exposed to one or more volatile precursors, which react and/or decompose on the substrate surface to produce the desired deposit. Chemical vapor deposition is divided into subcategories that are shown below.

Rapid Thermal CVD (RTCVD): Rapid thermal CVD (RTCVD) - CVD processes that use heating lamps or other methods to rapidly heat the wafer substrate. Heating only the substrate

rather than the gas or chamber walls helps reduce unwanted gas phase reactions that can lead to particle formation.

Hot Wire CVD (HWCVD): Hot wire CVD also known as catalytic CVD (Cat-CVD) or hot filament CVD (HFCVD). Uses a hot filament to chemically decompose the source gases.

Plasma-Enhanced CVD (PECVD): Plasma-Enhanced CVD (PECVD) - CVD processes that utilize plasma to enhance chemical reaction rates of the precursors. PECVD processing allows deposition at lower temperatures, which is often critical in the manufacture of semiconductors.

But in our experiment we use physical and chemical methods to synthesize ZnO nanostructures, In physical technique we oxidize Zn foils (annealing the Zn foil in rang of 200 to 800^{o}C) at different times (1 to 3 hours). In chemical method we find out ZnO nanostructure in Zn-C dry cell, this nanostructures formed due to chemical reaction between electrolyte and surface of Zn-C dry cell container (this is mead by Zn and it is act as anode of C-Zn dry cell) apart from this we use mechanical alloying method to synthesize Zn/Al_2O_3 nanocomposite. In this we use oxidized Zn foil (at 800^{o}C) and Al powder in proper stoichiometric proportion. This Zn and Al mixture are milled in ball milling for 30 hours. The characterization of ZnO nanostructure and Zn/Al2O3 nanocomposite are done by SEM, EDX, XRD and DSC.

CHAPTER 3

EXPERIMENTAL

3.1 EXPRIMENTAL

3.1.1 Synthesis of ZnO Nanostructure by oxidation techniques

3.1.2 Find the ZnO nanostructure in Zn-C dry cell

3.1.3 Synthesize of metal matrix nano composite by mechanical alloying

3.2 Experimental Instruments

3.2.1 Scanning electron microscopy

3.2.2 Energy Dispersive X-Ray Spectroscopy

3.2.3 Differential scanning calorimetry

3.2.4 X-ray diffraction techniques

3. EXPRIMENTAL:

In our experiment Zinc oxide nanostructure is synthesize by oxidation and chemical techniques. Apart for synthesize of ZnO nanostructures we also synthesize the metal matrix nano composite by mechanical alloying for this we use ZnO (which is synthesize by oxidation of pure Zn) and Aluminum powder.

3.1.1 Synthesis of ZnO Nanostructure by Oxidation Technique:

In this experiment pure Zn (foil or powder) was taken in silicon crucible, the crucible size is average 1.5cm in diameter (cone shape) 2.5cm in depth. The crucible which contain a Zn (foil or powder) is put in Furnace, and switch on the furnace the temperature reach to say ten temperature (200^oC, 300^oC, 400^oC, 500^oC, 600^oC, 700^oC, 800^oC and 900^oC) and hold the temperature for 1 and 2 hour then switch off the furnace cool the Zn (foil or powder) by annealing after cooling the Zn color is change in to gray color it initial color is white color that indicate the ZnO nanorods is formed. This nanorods was characterizes by JEOL JSM-6480LV scanning electron microscope, EDX, DSC and XRD.

In this experiment we oxides both Zinc foils and Zinc powder at wares temperatures (200^oC, 300^oC, 400^oC, 500^oC, 600^oC, 700^oC, 800^oC and 900^oC) and wares times (1 or 2 hours). We oxides the zinc in the presents of common air atmosphere, for this we use muffler furnace.

3.1.2 Find ZnO Nanostructure in Zn-C Dry Cell:

First we collect the completely life time used Zinc -Carbon dry cell and cut into pieces and take out the outer Zn sheet (which is container of the cell), the inner surface of the Zn anode is contact with the electrolyte (mixture composed of manganese (IV) dioxide (MnO_2), ammonium chloride (NH_4Cl) and zinc chloride ($ZnCl_2$).) . The inner surface of the Zn anode sheet is reacted with electrolyte and form ZnO nanostructure this was characterized by scanning electron microscopy (SEM). The Zn-C dry cell anode and cathode is show in below figure.

Figure 3.1 A used Zn-C dry cell showing the zinc casing that serves as both the container and the negative terminal. The carbon or graphite rod positive terminal is surrounded by the electrolyte which is a mixture of MnO_2, NH_4Cl and $ZnCl_2$.

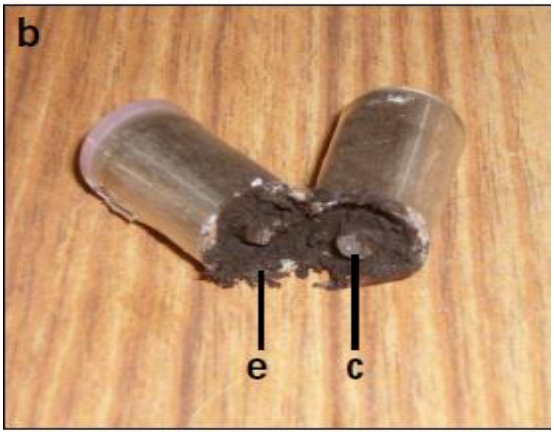

Figure 3.2 e-Electrolyte c- the carbon electrode

Figure 3.3 An opened Zn-C dry cell.

3.1.3 Synthesize of Metal Matrix Nano Composite by Mechanical Alloying:

We synthesize the Zn/Al_2O_3 metal matrix nano composite by using mechanical alloying technique, in this we use ZnO foils (which is made by oxidation of Zinc foils) and aluminum powder. In this experiment we take ZnO foil and Al powder.

$$3ZnO+2Al \rightarrow Al_2O_3+3Zn$$

We take balls to charge weight ratio as 10:1. The charge was put in a stainless steel vial and chrome steel balls were used for ball milling. The milled powder was characterized by XRD, SEM and DSC.

3.2 Experimental Instruments

3.2.1 Scanning Electron Microscopy:

A scanning electron microscope (SEM) is a type of electron microscope that images a sample by scanning it with a high-energy beam of electrons in a raster scan pattern. The electrons interact with the atoms that make up the sample producing signals that contain information about the sample's surface topography, composition, and other properties such as electrical conductivity. SEM can produce very high-resolution images of a sample surface, revealing details about less than 1 to 5 nm in size. Due to the very narrow electron beam, SEM micrographs have a large depth of field yielding a characteristic three-dimensional appearance useful for understanding the surface structure of a sample.

Fig.3.4: JEOL JSM-6480LV SEM.

In most of the applications, the data collected is over a pre selected area of the sample surface and following this, a 2D image is generated that shows the various spatial variations. Conventional SEMs with a magnification range of 20X-30000X with a spatial resolution of 50-100 nm can scan areas which vary from 1 cm to 5 μm in width. SEMs also have the ability to analyse particular points as can be seen during EDX operations which help in determining the chemical composition of the sample concerned [33].

The internal arrangement of SEM is shown below and SEM have following components

- Electron Source ("Gun")
- Electron Lenses
- Sample Stage
- Detectors for all signals of interest
- Display / Data output devices
- Infrastructure Requirements:

a) Power Supply

b) Vacuum System

c) Cooling system

d) Vibration-free floor

e) Room free of ambient magnetic and electric fields.

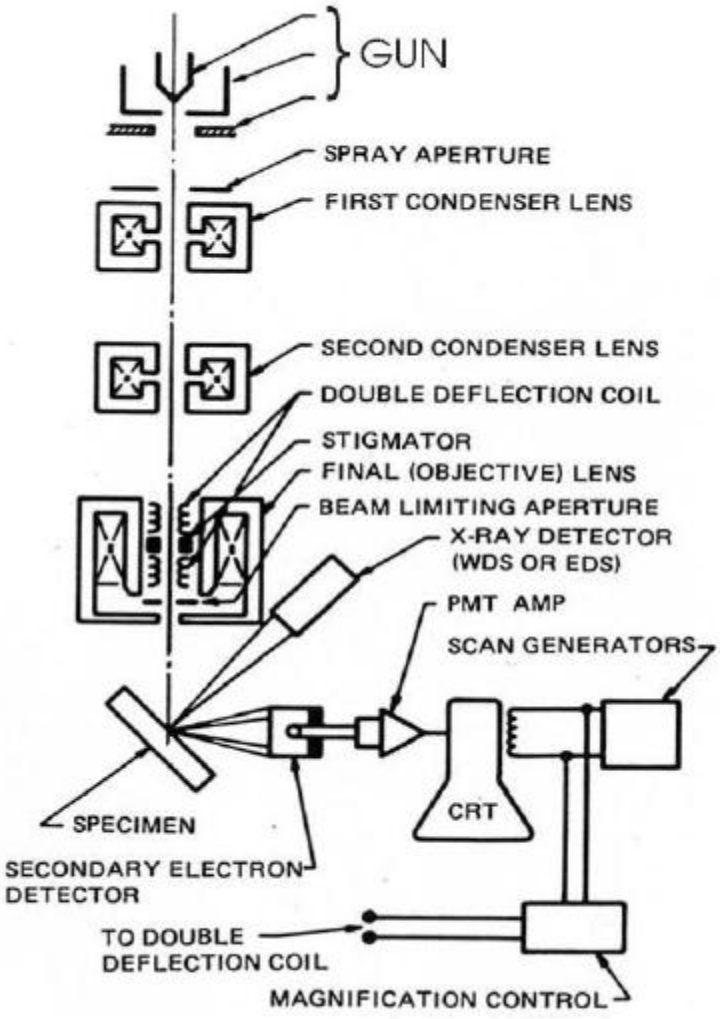

Fig.3.5: Schematic Diagram of Electron and x-ray optics of combined SEM- EPMA

3.2.2 Energy Dispersive X-Ray Spectroscopy:

Energy-dispersive X-ray spectroscopy (EDS or EDX) is an analytical technique used for the elemental analysis or chemical characterization of a sample. It is one of the variants of X-ray fluorescence spectroscopy which relies on the investigation of a sample through interactions between electromagnetic radiation and matter, analyzing X-rays emitted by the matter in response to being hit with charged particles. Its characterization capabilities are due in large part to the fundamental principle that each element has a unique atomic structure allowing X-rays that are characteristic of an element's atomic structure to be identified uniquely from one another [34,44].

3.2.3 Differential Scanning Calorimetry:

Differential scanning calorimetry or DSC is a thermo analytical technique in which the difference in the amount of heat required to increase the temperature of a sample and reference is measured as a function of temperature. Both the sample and reference are maintained at nearly the same temperature throughout the experiment. Generally, the temperature program for a DSC analysis is designed such that the sample holder temperature increases linearly as a function of time. The reference sample should have a well-defined heat capacity over the range of temperatures to be scanned [36].

Figure 3.6 Differential Scanning Calorimetry.

3.2.4 X-ray diffraction techniques:

X-ray diffraction (XRD) is a non-destructive type of analytical technique which provides valuable insight about the lattice structure of a crystalline substance like unit cell dimensions, bond angles, chemical composition and crystallographic structure of natural and manufactured materials. XRD is based on the principle of constructive interference of x-rays and the sample concerned which should be crystalline. The x-rays which are generated by a CRT are filtered, collimated and then directed towards the sample. The interaction that follows produces constructive interference based on Bragg"s law which relates wavelength of the incident radiations to the diffraction angle and lattice spacing [37].

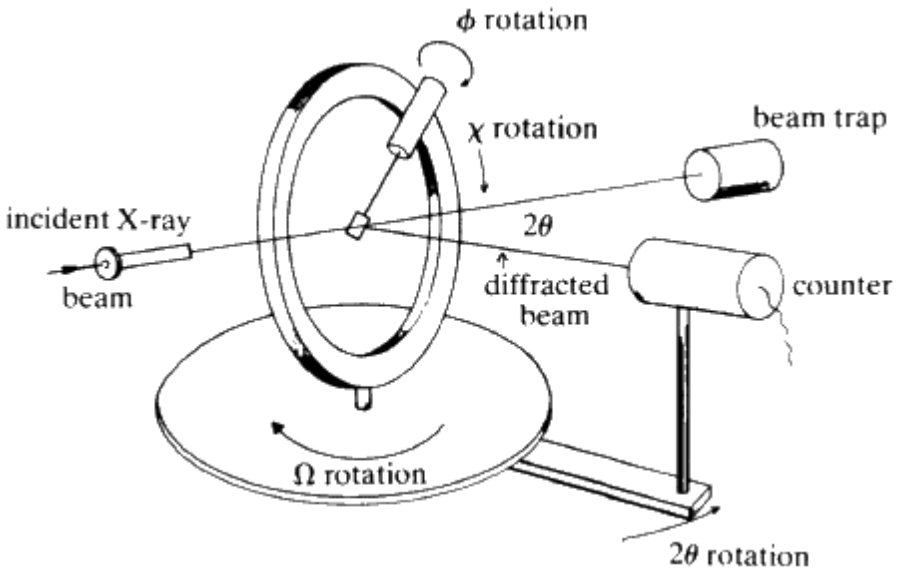

Figure.3.7: Schematic Diagram of a 4-Circle Diffractometer.

Image courtesy of the International Union of Crystallography [37].

CHAPTER 4

RESULTS & DISCUSSION

4.1 Synthesis of ZnO nanostructures by oxidation techniques

4.2 Find the ZnO nanostructures in Zn-C dry battery

4.3 Syntheses the Zn/Al_2O_3 nanocomposite by mechanical alloying techniques

4 Results:

4.1 Synthesize of ZnO Nanostructures by Oxidation Techniques:

Pure Zn foils were oxidized at temperatures 200^{o}C, 300^{o}C, 400^{o}C, 500^{o}C, 600^{o}C, 700^{o}C, 800^{o}C and 900^{o}C and for various periods of time. We take Zn foils in silicon crucible. This silicon crucible is kept in a muffle furnace and heated at different temperatures and different times. The oxidized samples are analyzed using SEM, EDX and XRD. First we observed that Zn has a metallic lusture but after heating, the lusture of metallic Zn is lost and it starts to have a white coloured layer on it which is the typical colour of ZnO. This color change indicates the formation of ZnO on the metallic Zn surface.

From below SEM images we analyze that the formation of ZnO nanostructures depends on heating temperature and also the holding time. If heating temperature is high it indicates oxidation is more so nanorods is more likely to form but in the lower temperature range of 500-600^{o}C the ZnO structure formed is mainly nanorods, nanobelts, nanorings, nanoribbons nanoneedles, nanolaves and nanowires etc. Heating time also affects the ZnO structure. We also find ZnO nanostructure forming temperature at around 400^{o}C (near melting temperature 419^{o}C) below this temperature at 200^{o}C and 300^{o}C we do not find any oxidation of Zn foils taking place. The DSC results in Fig. 4.3(c) also reflect the same. Oxidation of Zn foil mainly starts from 200^{o}C or beyond.

From SEM image in Fig. 4.1 we not find ZnO nanostructure at 300^{o}C. It indicates that the Zn is not oxidized at 300^{o}C. The EDX analysis indicates that the Zn foil is 100 % Zn even after oxidation of the Zn foil at 300^{o}C for 2 hours. Nanostructures are forming on the Zn foil at temperatures beyond 400^{o}C.

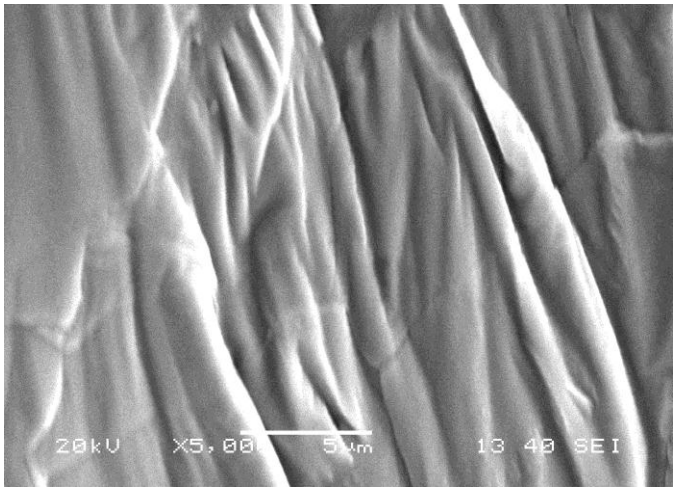

Fig 4.1 SEM image of Zn foil after annealing at 300^{o}C, at 2 hours this figure we not absorbed any nanostructure.

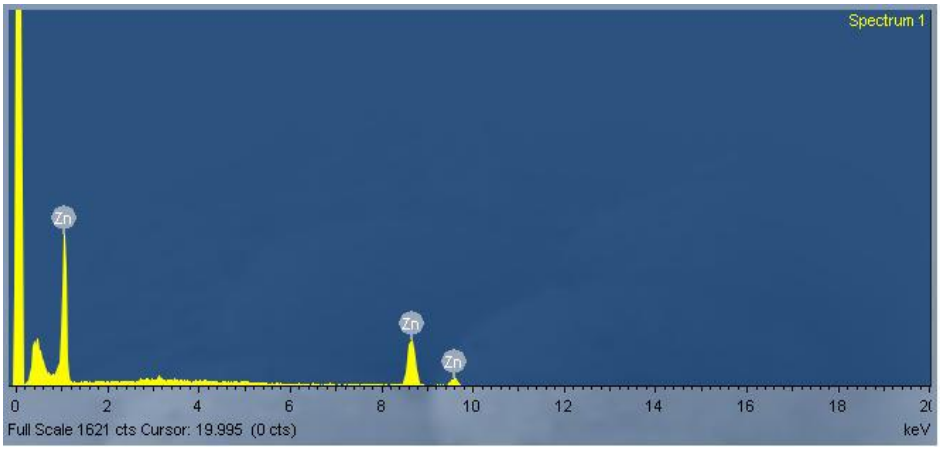

Fig 4.2 This is EDX figure of Zn foil after heating at 300^{o}C for 2 hours, this we not find O peaks.

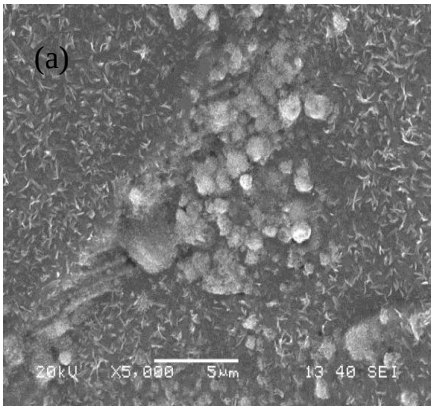

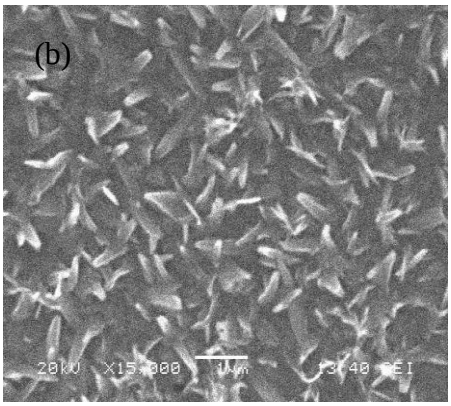

Fig 4.3(a-b) This figure shows SEM image of Zn foil after annealing at 400^{o}C for 2 hours. In this we are find ZnO nanorods. It means nanostructures are start to form from 400^{o}C.

DSC/TG ANALYSIS OF THE PURE ZINC SAMPLE:

The DSC/TG analysis of the pure Zn sample was done in order to find out the temperature at which oxidation of Zn starts and weight gain during oxidation as a function of temperature. The TG curve in below Fig. 4.3(c) shows a gain in weight by 1.09 %. At temperatures above 200^{o}C there is sign of weight gain which is due to the oxidation of Zn. At temperatures above 200^{o}C and up to 450^{o}C a weight gain mainly due to the oxidation of Zn could be seen. Below 200^{o}C hardly any gain in weight of Zn could be found. At 416.8^{o}C an endothermic peak corresponding to the melting temperature of Zn can be observed in the DSC plot.

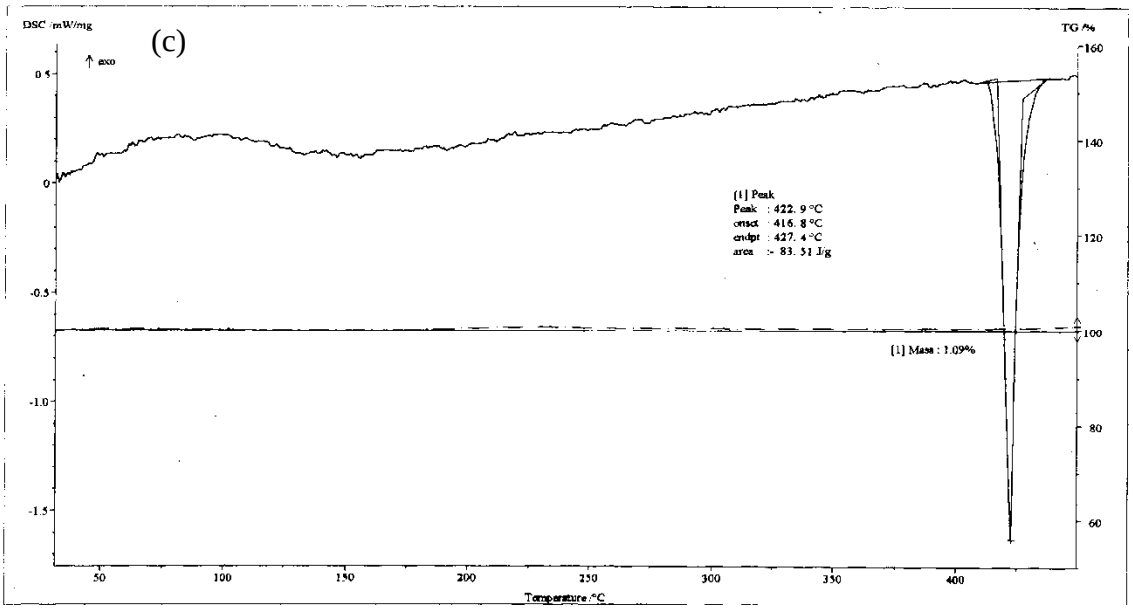

Graph 4.3(c) shows DSC/TG analysis of pure Zn foil in range up to 450^{o}C (30^{o}C/10 min) in air.

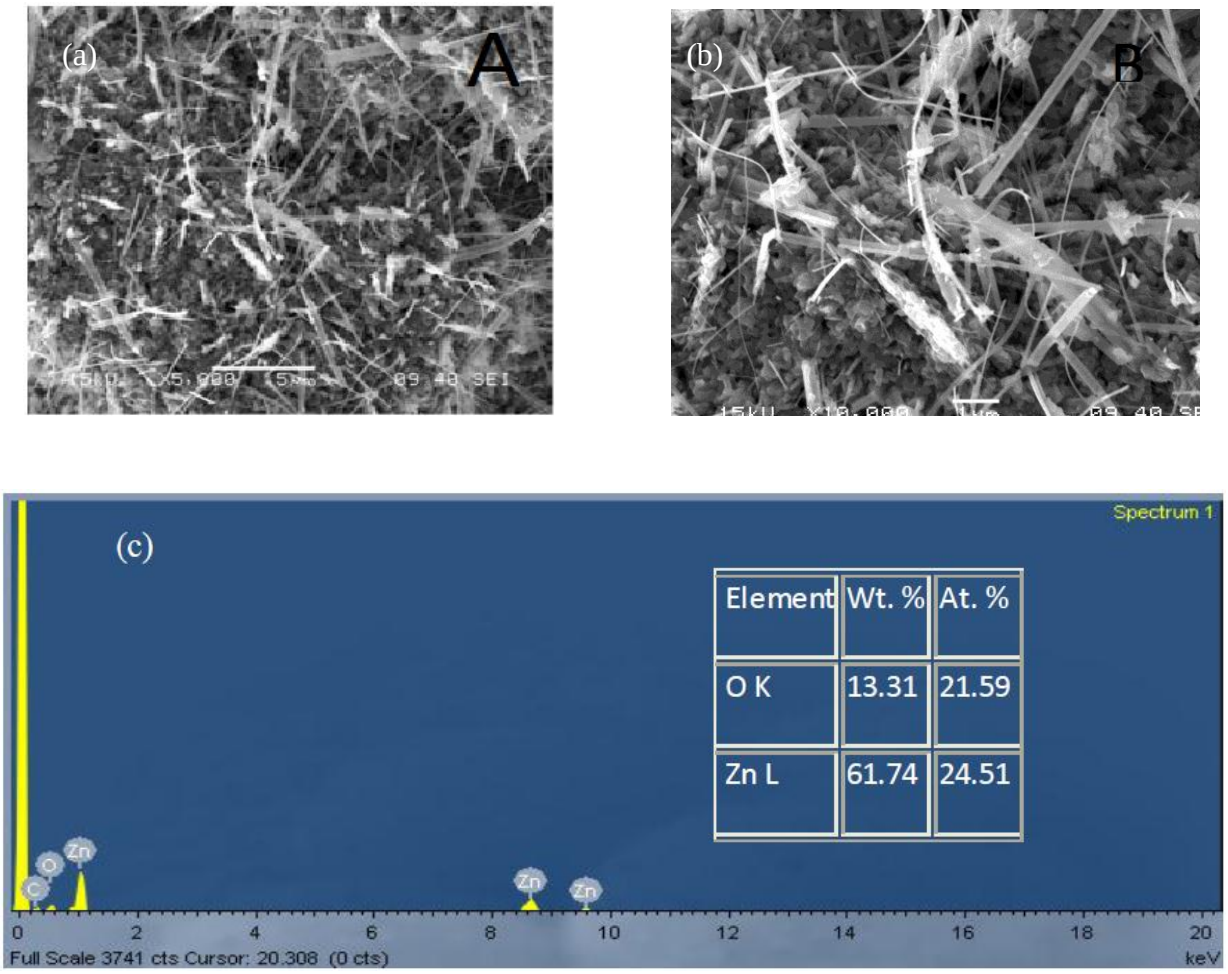

Fig 4.4 SEM images showing ZnO nanostructures obtained on Zn substrate after holding at 500°C for 2 h. (c) EDX of the obtained sample

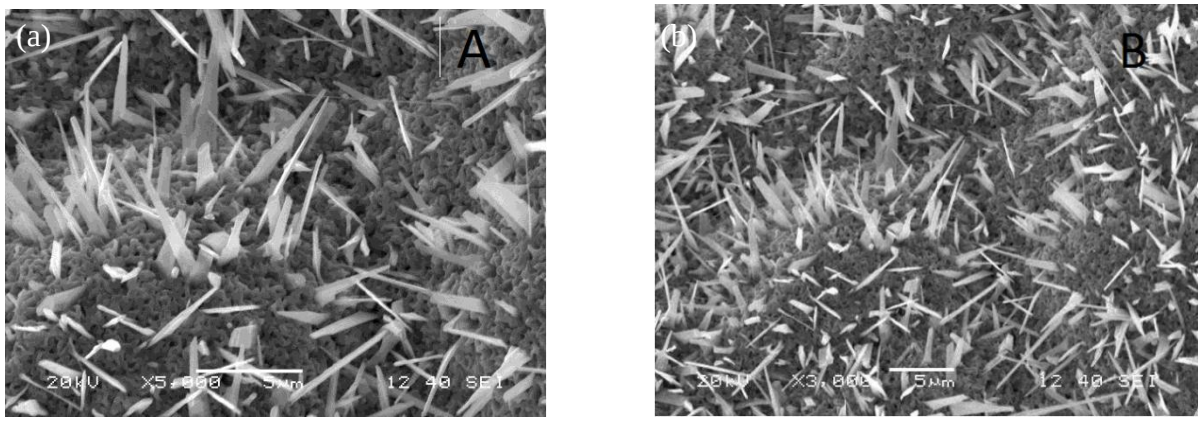

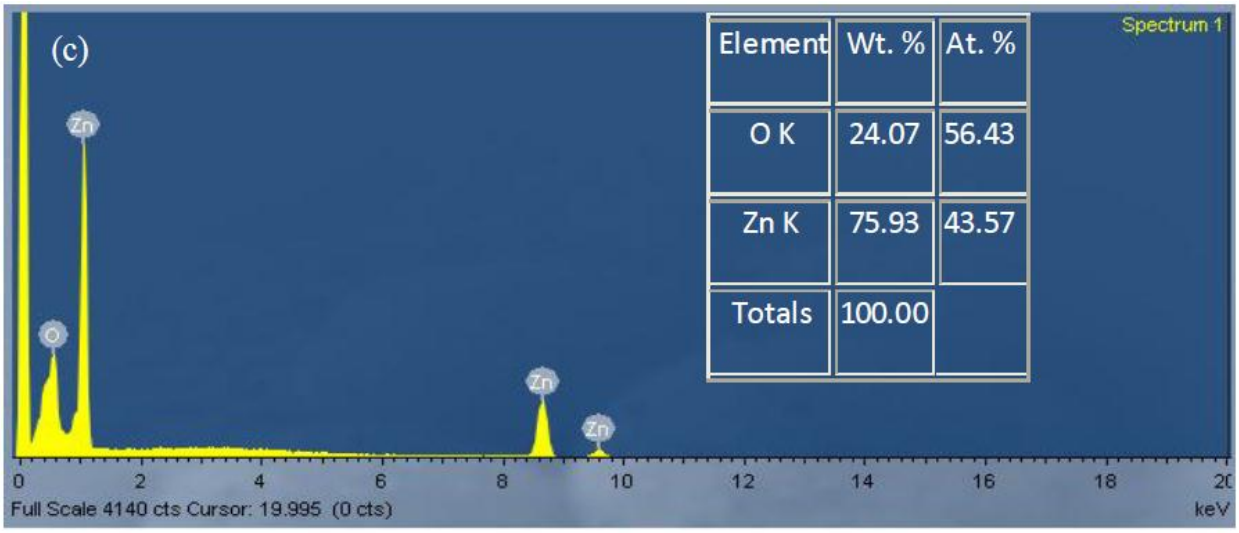

Fig. 4.5(a-b) SEM images of ZnO microstructures obtained on Zn substrate holding Zn at 700 °C for 2 h. (c) EDX of the protruded structure.

From above figure 4.4(c) and 4.5(c) we absorbed that oxygen percentage is increasing with heating temperature. Here we find that nanorods and nanoneedles like nanostructures this nanorods and nanoneedles are increasing with temperature. Temperature is high nanorods height is more and according to height width is decreasing from bottom to end tip. And also find that the number of nanorods is increasing with temperature. The nanorods and nanoneedles are formed in triangle shape and different nanorods in different height.

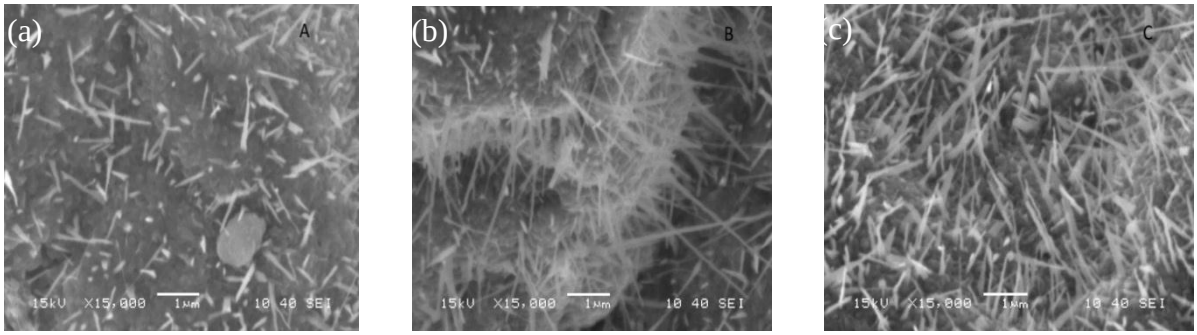

Figures 4.6(a-c) showing SEM images of Zn foil after annealing at same temperature (600^{o}C) at different times (a) for 1 h, (b) for 2 h and (c) for 3 h.

From above figures we analysis that ZnO nanostructures are depending on heating time. Heating time is more ZnO nanorods are more and height is increase with time width of nanorods are decrease. Heating time increase the shape of nanorods and nanoneedles come into triangular shape rods. But nanostructure mainly depends on heating temperature.

From the SEM image in Figs. 4(a-b) we can confirm that at the oxidizing temperature of 400^{o}C the surface of Zn shows the formation of ZnO structures. When Zn was held at 500^{o}C for 2 h the SEM images of the surface shows the formation of a wide range of ZnO nanostructures (Figs. 4.3(a-b)). EDX analysis of these nanostructures in Fig. 4.3(c) reveals that their composition is almost that of stoichiometric ZnO (21.59 at. % O and 24.51 at. % Zn). At the oxidizing temperature of 600^{o}C also we see that the surface of Zn is completely filled with nanostructures of ZnO (Figs. 4.4 (a-b)). As can be seen from the SEM image in Figs. 4.4 (a-b) there is a wide range of nanostructures of ZnO on the Zn surface. ZnO having structures such as nanowires, nanobelts and nanoribbons could be seen in the samples oxidized at 500 and 600^{o}C (Figs. 5(a-b) and Figs. 4.4(a-b)). On the other hand the oxidation of Zn at 700^{o}C does not show nanostructured ZnO (Figs. 4.5(a-b)). There is a gradual increase in the size of the ZnO structure with further increase in temperature. Figs. 4.7(a-b) are the SEM images of Zn oxidized at 800^{o}C for 2 h. Nanostructures of ZnO could not be seen at this oxidizing temperature. The EDX analysis in Fig. 4.5(c) of the ZnO microstructure formed by oxidizing Zn at 700^{o}C for 2 h shows that the at. % of Zn is 43.57 % and that of O is 56.43 %, suggesting that highly stoichiometric ZnO is formed at this temperature. The EDX spectrum shows that only O and Zn elements are detected, confirming the formation of pure ZnO.

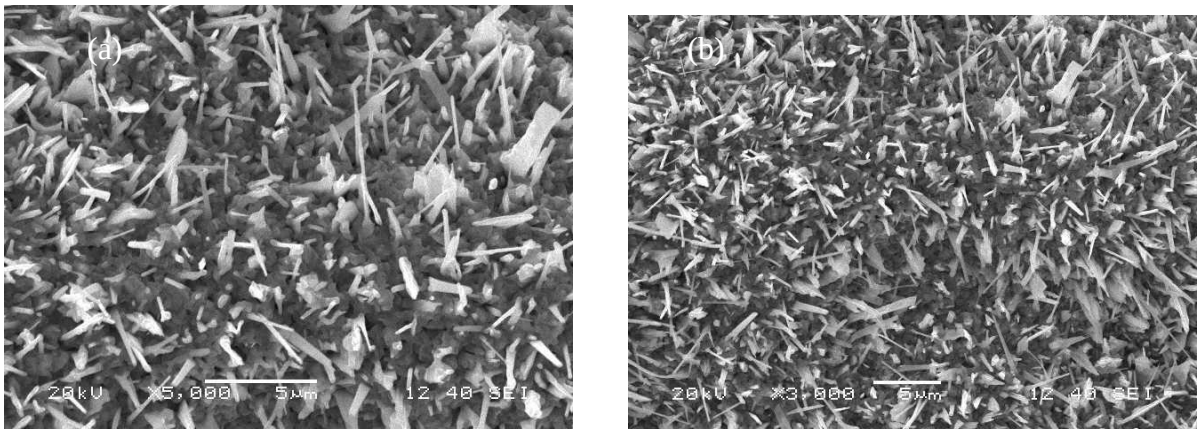

Fig. 4.7(a-b): SEM images showing ZnO structures obtained on holding Zn for 2 h at 800°C.

4.2 Find the ZnO nanostructures in Zn-C dry battery

In Zn-C dry cell the Zn container act as negative terminal (anode), the carbon (graphite) acts as a positive terminal (cathode). The Zn anode inner surface is contact with electrolyte, the electrolyte is mixture of manganese (IV) dioxide (MnO_2), ammonium chloride (NH_4Cl) and zinc chloride ($ZnCl_2$). The inner surface of Zn (anode) is react with electrolyte and form ZnO nanostructure.

First the atom of Zn on the Zn electrode is oxidized to Zn^{2+} ion, liberating two electrons. These two electrons was taken by NH^{4+} and form NH_3 and relies H_2 gas, this NH3 and Zn2+ form zinc di ammonia. This chemical reaction was show below.

$$Zn(s) \rightarrow Zn^{2+} + 2^{e-}$$

$$2NH^{4+}(aq) + 2^{e-} \rightarrow H_2(g) + 2NH_3(aq)$$
$$2MnO_2(s) + H2(g) \rightarrow Mn2O3(s) + H_2O(l)$$

$$Zn^{2+} + 2NH_3(aq) \rightarrow Zn(NH_3)_2{}^{2+}(aq)$$

The MnO_2 reacts with H_2 and gives water and Mn_2O_3. This H_2O reacts with $Zn(NH_3)_2{}^{2+}$ (aq) and form ZnO. The all above chemical reaction can also Wright as

$$Zn(s) + 2MnO_2(s) + 2NH^{4+}(aq) \rightarrow Mn_2O_3(s) + Zn(NH_3)_2{}^{2+}(aq) + H_2O(l)$$

One of the reactions that could lead to the formation of ZnO in the Zn electrode is:

$$H_2O(l) \rightarrow H^+(aq) + (OH)^-(aq)$$

$$Zn(s) + 2OH^-(aq) \rightarrow ZnO + H_2O + 2e^-$$

A reaction of this type is likely to result in the formation of ZnO. It has also been reported earlier by Wu et al. [8] that $Zn(OH)_4{}^{2-}$ decomposes and forms a nucleus for the growth of ZnO crystals when the solution was placed into the 50°C water bath.

This sample was characterized by SEM the images was shown below

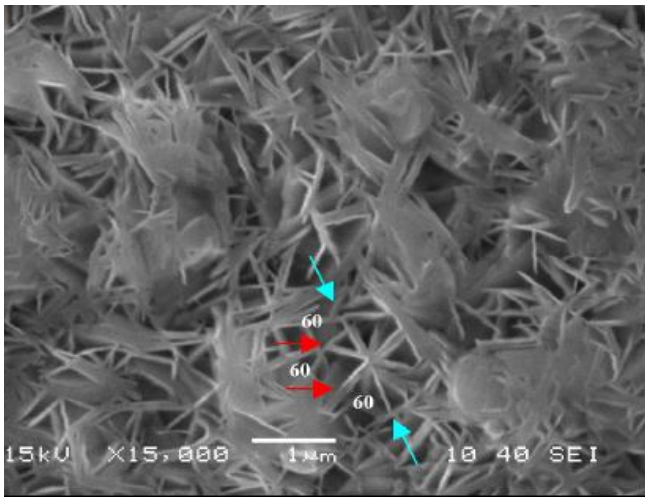

Figure 4.8 SEM image of the surface of the Zn electrode of a Zn- C dry cell. Arrows: ZnO structure illustrating clearly the SRAS distribution.

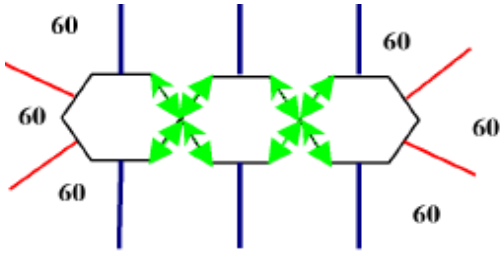

Figure 4.9 Schematic showing the relative position of the SRAS.

The ZnO prefers to grow along the c-axisand the (0001) plane. The first formed ZnO stem provides its six prismatic planes as the platforms for the later growth of the branches. The process of formation of the hierarchical structure starts with the generation of the nanorods. The nanorods after their formation are aligned together and fused into a wall to form the PRAS. For the rods located on each end of a PRA, two of their six planes cannot act as a platform due to the spatial barrier (marked as green lines with arrow heads at both ends in the schematic diagram in Figure 4.8). On the contrary, for the rods located inside a PRA, only two of the six planes can act as the platform for the later growth of the SRAS (refer to Figure 4.9) [38,39].

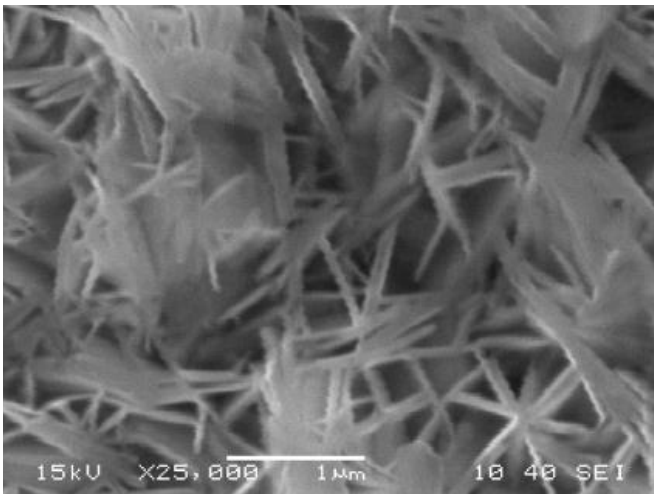

Figure 4.10 SEM image of the surface of the Zn electrode of a Zn-C dry cell.

From figures 4.10 we analyze that each hierarchical structure of ZnO consists of many nanorod arrays as its secondary structure. From the magnified SEM image we can see symmetrical rod-arrays. These arrays of rods comprising the hierarchical structure can be divided into two categories, namely primary rod arrays (PRAS) and secondary rod arrays (SRAS) [40]. The PRAS are formed into a line while the SRAS look like branches coming out of the PRAS. SRAS which are located at both ends of the PRAS form an angle of 60° with each other, while the SRAS located at the inner area of PRAS are parallel to each other. The tips of the ZnO rods in both PRAS and SRAS are pointed. According to previous work, the first formed stem can provide its six prismatic planes as the platforms for the later growth of the branches. The legs of the star like structures have a thickness of just less than 100 nm. The legs of the star-like structures preferentially grew along the [0001] direction [41,42]. The lengths of the legs are around 0.5 μm .

The EDX analysis of the ZnO structures is shown in below figure 4. In this the ZnO consist of Zn (at. % = 48.07 %) and O (at. % = 44.79 %) there is also the presence of a small amount of Cl (at. % = 7.14 %). The Cl present because the electrolyte composed of manganese (IV) dioxide (MnO_2), ammonium chloride (NH_4Cl) and zinc chloride ($ZnCl_2$). The Cl come from ammonium chloride (NH4Cl) and zinc chloride (ZnCl2) in the electrolyte. So this ZnO is not very pure and also have some amount of Cl. The EDX analysis fig 5 is shown below figure.

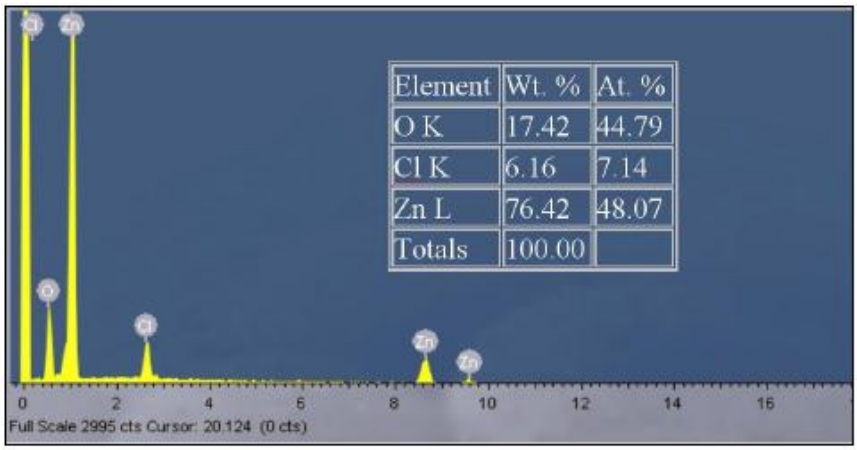

Fig 4.11 shown EDX analysis of ZnO in Zn-C dry cell.

Initially the formation of ZnO is very slow and gradually the small ZnO particles fuse to form the ZnO nanorods. First the nanorods were formed along the [0001] direction. Then, the formed rods aggregated side by side to reduce their surface energy and finally fused to form a wall. However, when the rate of the growth of ZnO structures became very rapid, the prismatic planes of the ZnO rods that have already formed act as the substrates to compensate the rapid growth rate. This is the stage when the secondary rod arrays are formed. The schematic in Figure 4.12 shows the details of how the PRAS and SRAS are formed. the below figure shows SRAS formation on PRAS. With 60^{o} angle.

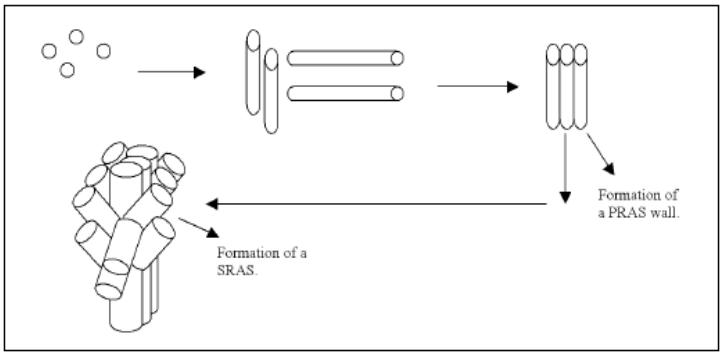

Figure 4.12 showing the details of how the PRAS and the SRAS grow and the formation process of the hierarchical structure.

Apart from hierarchical structure we find rod like structure of ZnO. In figure 4.13(a-d) we show this rod like structure of ZnO.

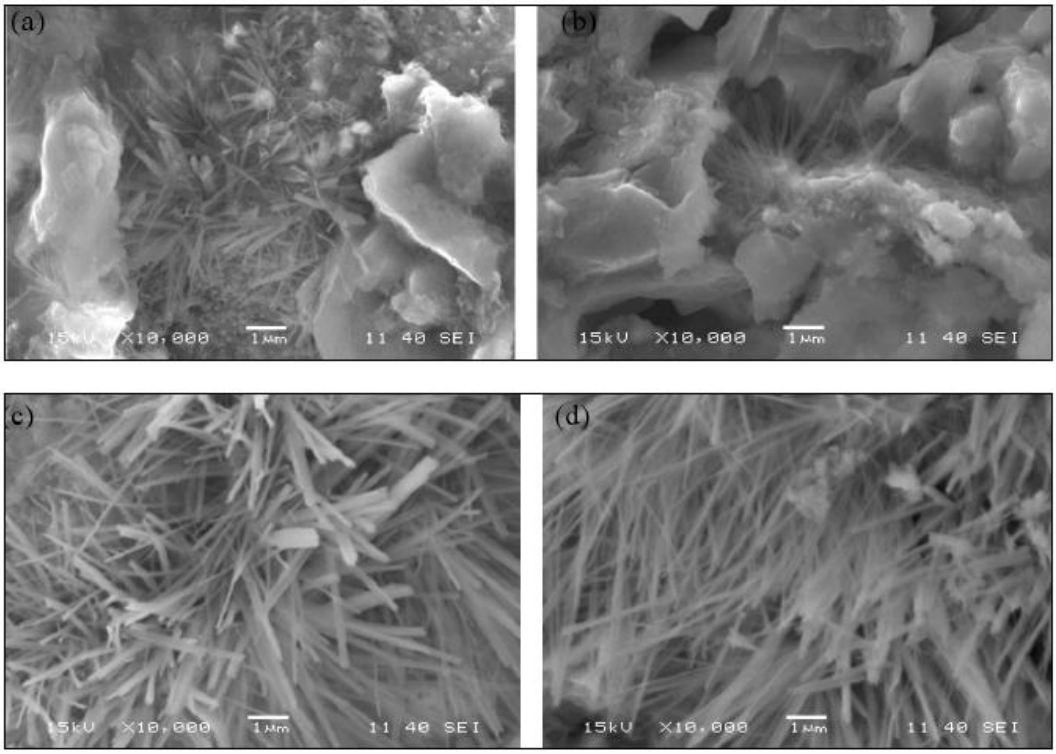

Figure 4.13(a-d) SEM images of Zn casings of various used Zn-C dry cells showing the formation of ZnO nanorods.

The ZnO nanorods also not pure. It consist of some other material in little amount that could be found by EDX analysis of the nanorods. The EDX analysis shows presence of other elements such as Cl, K and Pb. The atomic % of oxygen in the nanostructures is very high. In the samples the atomic % of oxygen was 43.45 whereas the atomic % of zinc was 23.38. This clearly proves that the nanostructures are not of high purity ZnO and also not stoichiometric. Apart from this, elements like Cl (11.59 atomic %) were also seen in the ZnO structure. The EDX result is shown below in Fig. 4.14.

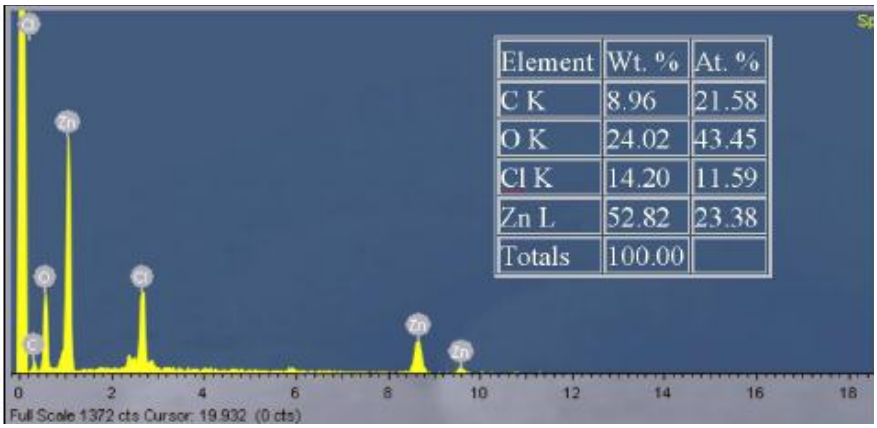

Figure 4.14 EDX analyses of the ZnO Nano rods formed in the Zn electrode of a Zn-C dry cell.

4.3 Syntheses the Zn/Al_2O_3 Nanocomposite by Mechanical Alloying Technique

In our experiment we syntheses the Zn/Al_2O_3 nano composite by mechanical alloying method, in this process displacement reaction takes place between Al and ZnO and form Al_2O_3 and Zn. This reaction is given below.

$$2Al(s) + 3ZnO(s) = Al_2O_3(s) + 3Zn(s)$$

From XRD data in Fig. 4.15 we conform that some ZnO peaks are dispread and Zn peaks are find with little shift in the peak and we find Al_2O_3 peaks with very little intensity. Below graph show the milled shape at 10h and 30h, in 30h graph we can find that Al_2O_3 peaks are form at 65.157^o and 86.770^o this indicating that displacement reaction between Al and ZnO. This peak intensity is very small.

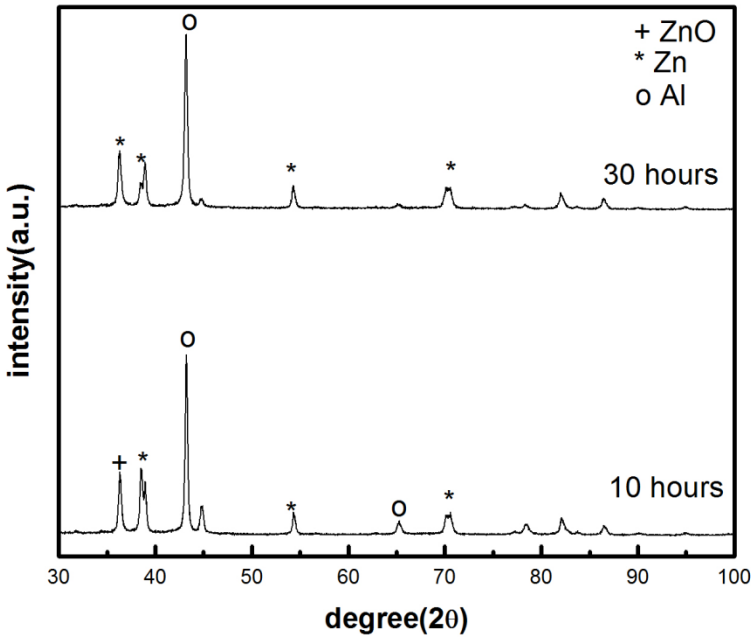

Figure 4.15 show the XRD peaks of milled powder of ZnO foil and Al powder at 30 hours and 10 hours.

From graph 4.16 we also observed that Zn peaks are present at 10h this indicates the inner part of Zn foils are not oxides at 800^{o}C for 2 hours. Form above graph we can find the peak at 36.015^{o} is shifted to 36.335^{o} it indicating that ZnO peak is disappeared at 36.015^{o} and Zn peak is formed at 36.335^{o} this is the symbol for displacement reaction take place in this process.

Apart from this we can also fined $ZnAl_2O_4$ component from XRD analysis, $ZnAl_2O_4$ component is form due to unreacted ZnO. From this component indicates that the displacement reaction is exothermal reaction we need supply thermal energy to unreacted ZnO to react completely. This graph is shown below. from graphs 4.2 we can observed that the intensity of Zn peaks are decreases, this decreases due to the partial dissolution of Zn in Al lattice as well as grain boundaries. Another possibility is that the Zn could disperse into the Al as insolated particles, having very small sizes which are practically undetectable by XRD [43].

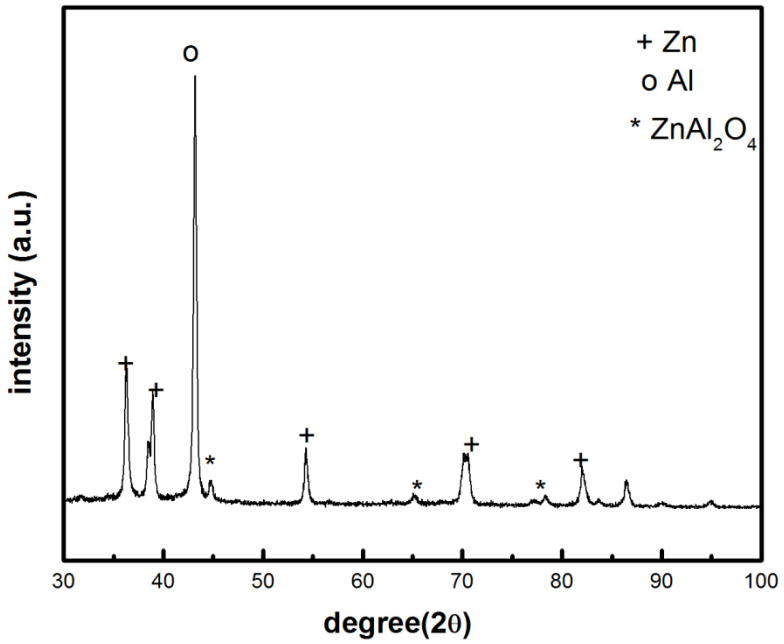

Figure 4.16 show 30 hours milled ZnO foil and Al powder XRD peaks from this we observed $ZnAl_2O_4$ peaks.

From DSC result of 10h milled sample. From DSC graph 4.17 the peak at 278.5^{o}C indicating endothermic, this peak is formed due to Zn micro scale practical's dissolving. The peak at 614.4^{o}C indicate the displacement reaction is exothermal reaction, the reaction is negative free energy (-ΔH). This indicates that the displacement reaction takes place at high temperature. To take displacement reaction between ZnO and Al_2O_3 we need to supply heat, this heat is getting in milling process and displacement reaction take place. We can analysis from DSC results of different time milled samples the exothermic peak is shifting towards low temperature side, this indicating that the displacement reaction takes place at increasing with milling time.

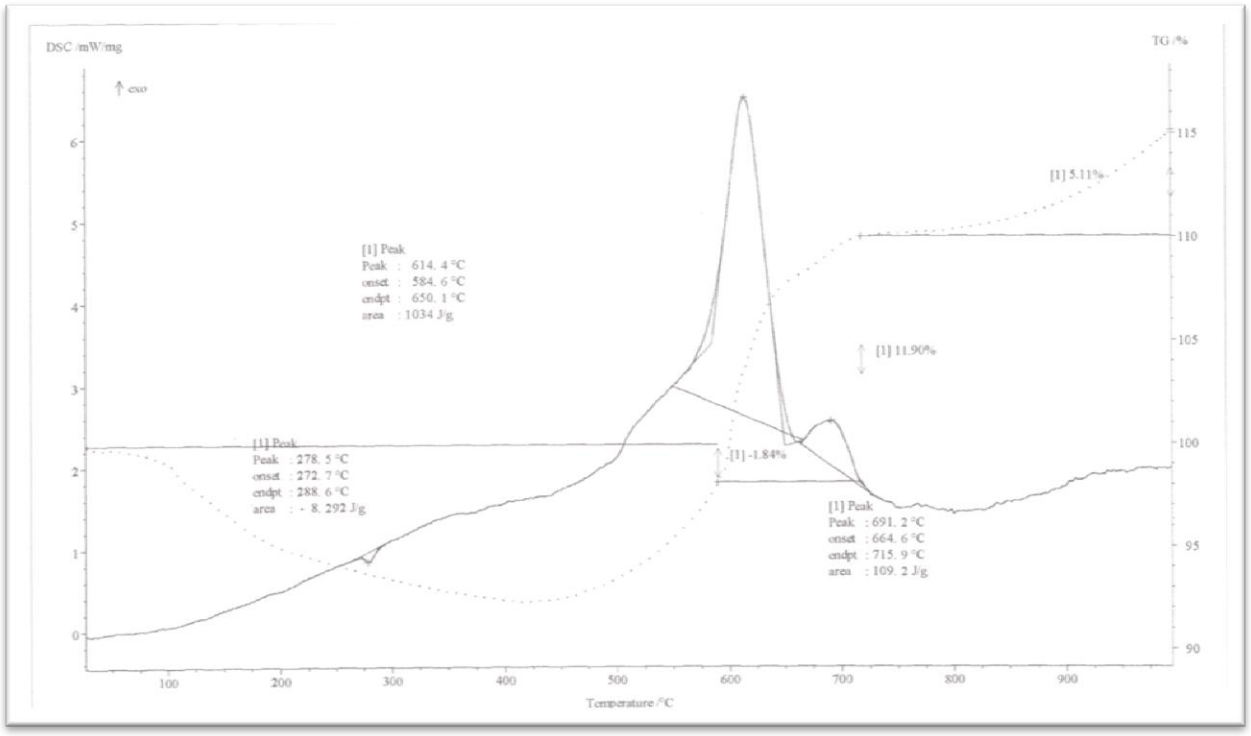

Figure 4.17 indicates DSC results of 10h milled ZnO foils and Al powder. (DSC done in Argon gas atmosphere, heated up to 1000^{o}C with 25^{o}C heat supply rate)

From below SEM images we analysis the formation of Zn/Al_2O_3 nanocomposite. Below figure 4.18 shows the SEM images of 5h, 10h, 15h, 20h, 25h, and 30h milled mixture of ZnO foil and Al powder, from this images we analyze that the ZnO foil is break in to micro scale rang practical's, at 5h the practical size is in micro scale rang the Al powder is already in micro scale rang. The practical's size is decreasing with milling time. After 30h milling the practical size is decreased into nanometer scale. The EDX analysis of milled sample is shown below figures from this we analyze that the oxygen percentage is increasing with milling time. The 30h milled powder has nano scale practical. This nano scale practical EDX analyses give the Al, Zn and O composition. This indicates nano composites are formed after 30h milling.

The below figure are belongs to 5h milled powder (ZnO and Al), from this images we can confirm that the practical's are in micro scale rang. The ZnO foils are break into order of micro scale rang. The Al powder is already in micro scale rang.

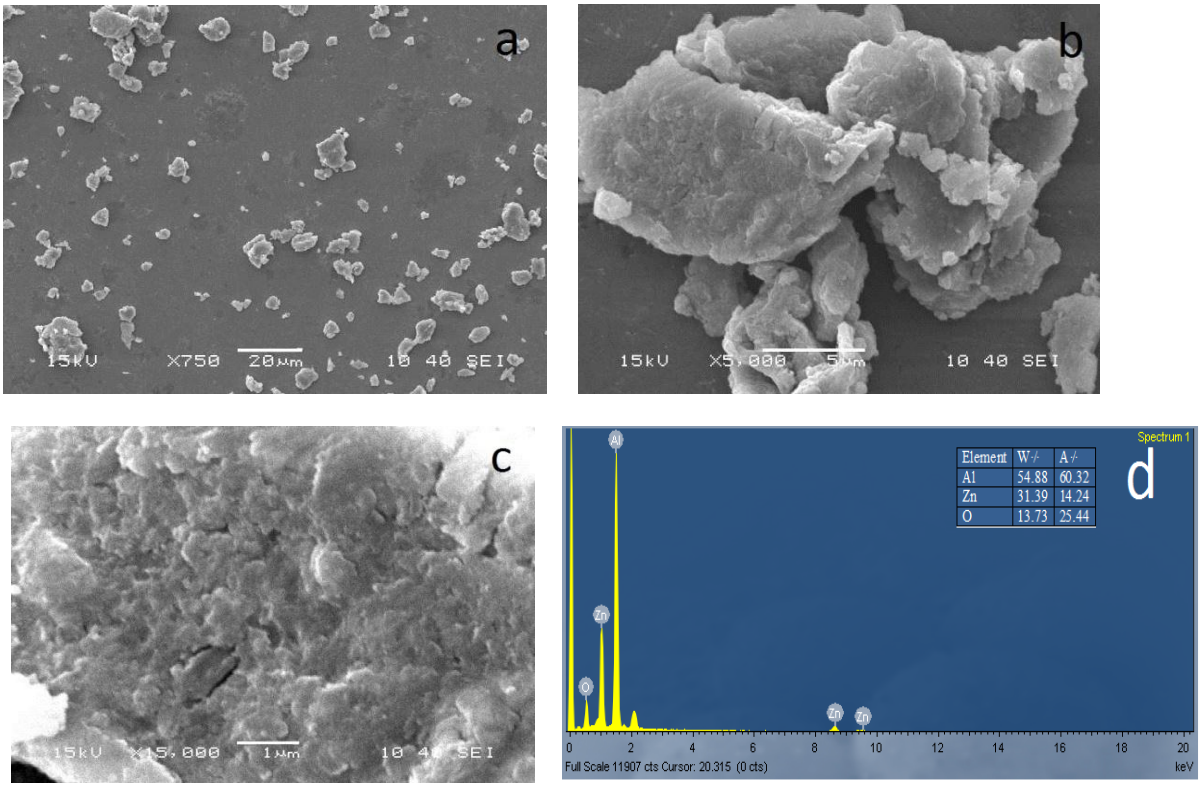

Figures 4.18 show the SEM images of ZnO foil and Al powder milled after 5 hours. Figure a), b), c) show SEM image of ZnO & Al milling with 750X, 5000X and 15000X revolutions. The fig. d indicates EDX analysis of 5h milled sample.

The below SEM images shows the 10 hours milled ZnO and Al powder from this we observed that the powder is still in micro scale rang but compare to 5h sample 10h sample size is decries. Form images we observed that the white spots indicating agglomeration of Al powder practices on oxidized Zn surface.

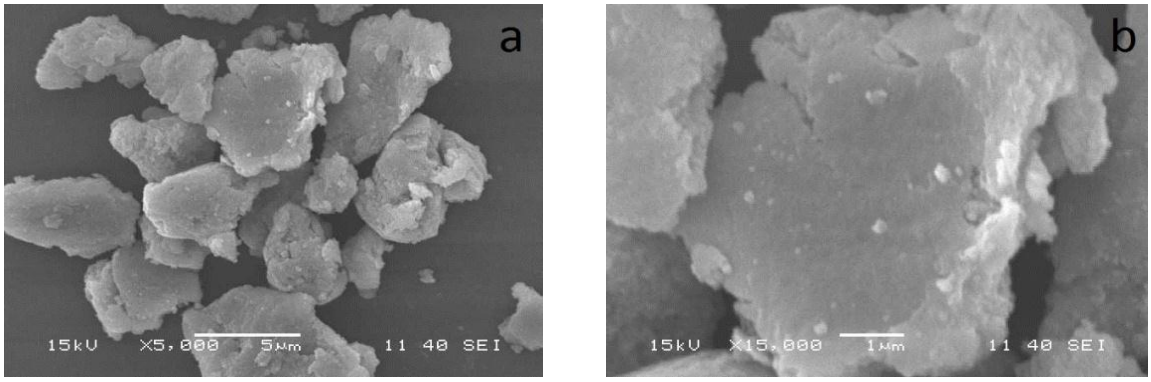

Figure 4.19(a-b) show SEM image of ZnO and Al 10 h milled sample at, a) 5000X, b) 15000X magnifications

The figures 4.20 shows the SEM images of 15h and 25h milled ZnO and Al mixture. Form this we analysis that the practical's size is reduced to 2 micro meter rang to 0.5 micro meter rang. From EDX data of 15h we analysis that the oxygen and Zn percentage is increase because the ZnO foil are breaking in to micro scale practical's t he inner part of oxidized Zn foil is not completely oxidized still it is in the form of Zn. So Zn percentage is increase. Oxygen percentage is increase indicates displacement is ready to start.

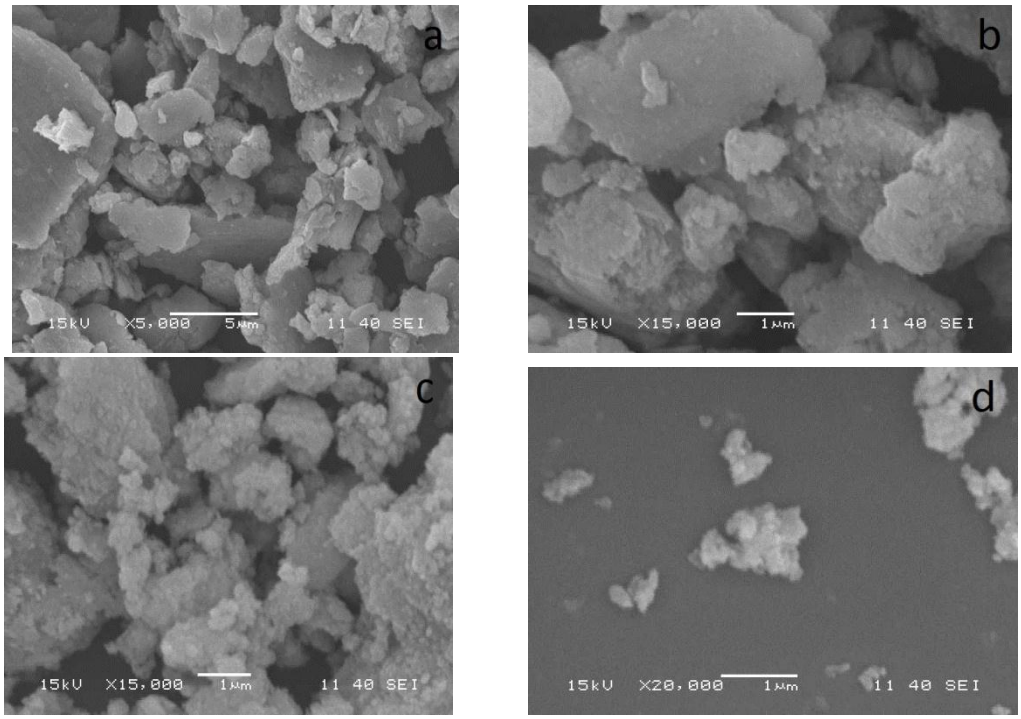

Figure 4.20 a) and b) give SEM image of 15h milled ZnO and Al mixture fig. a) At 5,000X, b) 15,000X magnification. Fig c) and d) gives SEM images of 25h milled ZnO and Al powder fig c) 15,000X, d) 20,000X magnification.

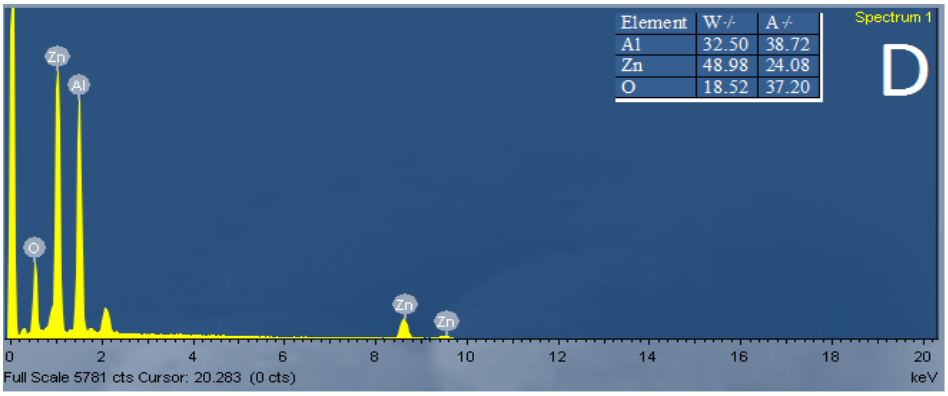

Figure 4.21 shows EDX analysis 15h milled oxidized Zn foil and Al powder.

Below figures 4.19 is SEM image of 30 hours milled oxidized Zn foil and Al powder, from this image we find that the sample practical size decreased into nano meter scale and we also find from EDX analysis the oxygen percentage is increase and Zn percentage is slightly decrease. This indicates dissolution of Zn in Al lattice as well as grain boundaries. The oxygen increase indicates the displacement reaction takes place. From figure (b) we clearly observed that nano scale particles are forming.

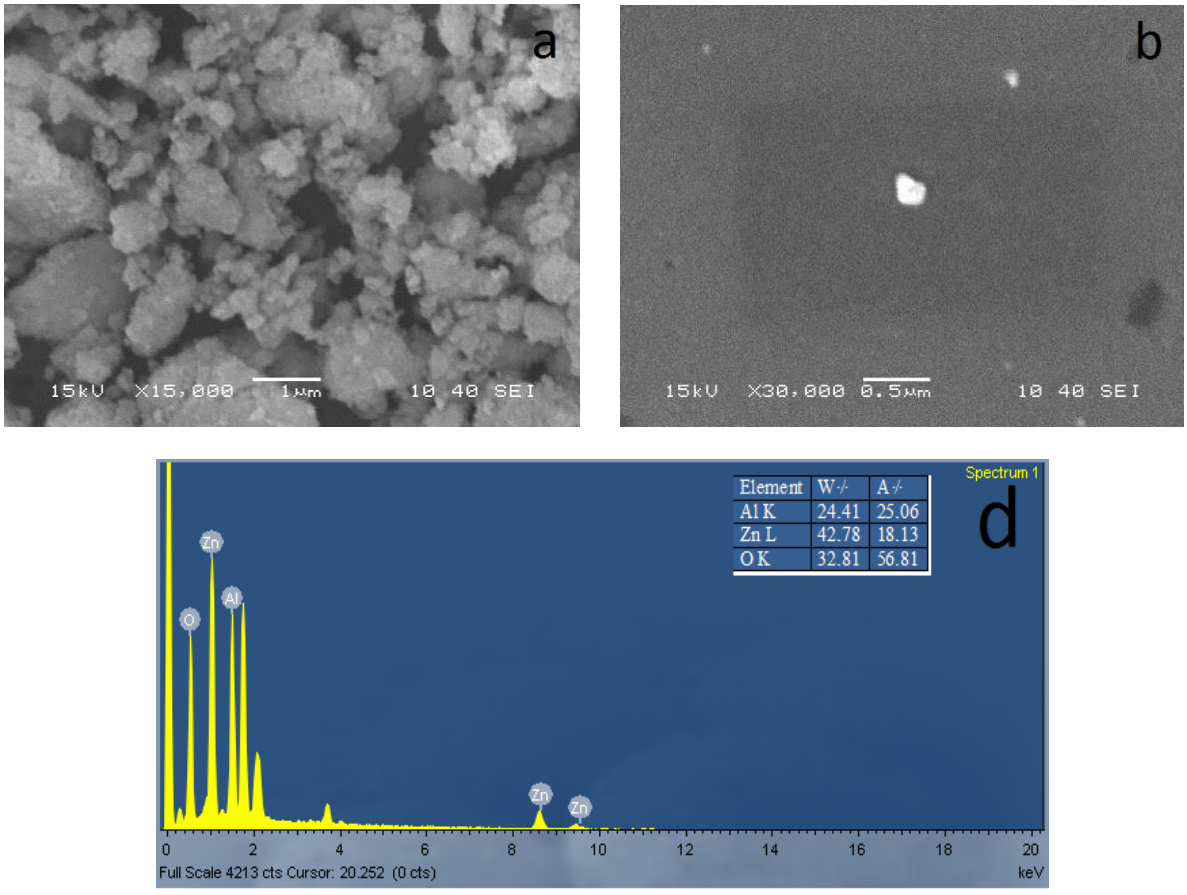

Figure 4.22 (a-b) indicates SEM images of 30h milled ZnO and Al mixture at 15,000X and 30,000X magnification. Figure (c) shows EDX analysis 30 h milled oxidized Zn foil and Al powder.

The EDX analysis is done for nano scale practical. In this analysis we find the Al, Zn, O components in good ratio this indicate Zn/Al_2O_3 composite is form after 30 hours milling of oxidized Zn foil and Al powder. This EDX figure is shown below.

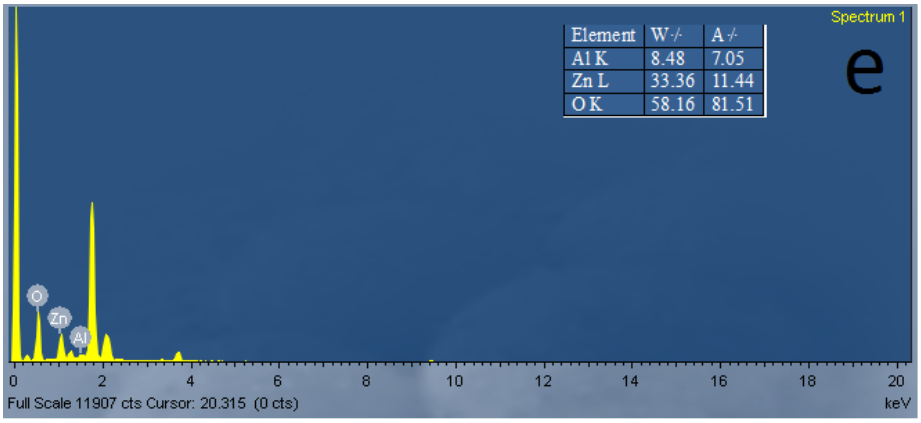

Figure 4.23 EDX analysis of nano scale rang of 30h milled ZnO and Al mixture.

CHAPTER 5

CONCLUSIONS

CONCULSIONS:

A Simple technique for ZnO nanostructure synthesis has been used here successfully. Different ZnO nanostructures are synthesized by simple techniques for different applications. Here we use oxidation technique, it is very simple, no complexity and without catalyst technique to synthesis a wide range of ZnO nanostructures. We also find that the nanostructure density depends on heating time and temperature. Oxidation technique is very simple and low cost method to synthesize the ZnO nanostructures.

We also find ZnO nanostructure in Zn-C dry cell. Here it is clear indication of the fact that the Zn casing of the Zn-C dry cell gets oxidized due to the electrochemical reaction with the electrolyte of the cell forming ZnO nanostructures. The nanostructures of ZnO are of various shapes. Rod-like, wire-like and star-like nanostructures of ZnO have been found in the surface of the Zn electrode of the Zn-C dry cell that is in contact with the electrolyte. The ZnO nanostructures do not have very high purity and are also not highly stoichiometric.

Apart from this we tried to synthesize Zn/Al_2O_3 nanocomposite by mechanical alloying (MA) technique. In this Zn foils oxidized at 800^oC and Al powder were milled. The Al_2O_3 particles that formed during milling are very small and have low crystallinity structure (amorphous structure) Mechanical alloying is good technique to synthesize the bulk amount of Zn/Al_2O_3 nanocomposite. From XRD, SEM and EDX data we conclude that displacement reaction takes place between ZnO and Al and from Zn/Al_2O_3 nanocomposite can be formed.

CHAPTER-6
REFERENCES

REFERENCES:

[1] J.J. Wu, S.C. Liu, Controlled growth of well-aligned hierarchical ZnO arrays by a wet chemical technique, Adv. Mater. 14 (2002) 215.

[2] D.B. Xiao, L. Xi, W.S. Yang, H.B. Fu, Z.G. Shuai, Y. Fang, J.N. Yao, J. Low. Dimensional Aggregates from Stilbazolium-Like Dyes, Amgewandte Chemie. Volume 43, Issue 31, pages 4060–4063, August 6, 2004.

[3] Z.Y. Tian, Y. Chen, W.S. Yang, J.N. Yao, L.Y. Zhu, Z.G. Shuai, Angew. Growth, morphology and optical properties of tris, Chem. 116 (2004) 4152.

[4] Xu CX, Sun XW, Chen BJ, Shum P, Li S, Hu X. J Zinc oxide nanowires and nanorods fabricated by vapour-phase . Appl Phys 2004;95:661–6.

[5] Y.C. Kong, D.P. Yu, B. Zhang, W. Fang, S.Q. Feng, Ultraviolet-emitting ZnO nanowires synthesized by a physical vapor deposition Appl. Phys. Lett. 78 (2001) 407.

[6] Y.W. Heo, V. Varadarajan, M. Kaufman, K. Kim, D.P. Norton, F. Ren, P.H. Fleming, Periodic array of uniform ZnO nanorods by second-order self-assembly, Appl. Phys. Lett. 81 (2002) 3046.

[7] Y.W. Wang, L.D. Zhang, G.Z. Wang, X.S. Peng, Z.Q. Chu, C.H. Liang, J. Cryst. Catalytic growth of semiconducting zinc oxide nanowires and their photoluminescence properties Journal of Crystal Growth 234 (2002) 171–175.

[8] P. Yang, H. Yan, S. Mao, R. Russo, J. Johnson, R. Saykally, N. Morris, J. Pham, R. He, H.J.Choi, Adv. Funct. Mater. 12 (2002) 323.

[9] Z.W. Pan, Z.R. Dai, Z.L. Wang, "Nanobelts of semiconducting oxides",Science 291 (2001) 1947.

[10] Y. Wu, P. Yang, J. Am. Chem. One-Dimensional Nanostructures as Subwavelength Optical Elements, Soc. 123 (2001) 3165.

[11] S.Y. Han, D.H. Lee, Y.J. Chang, S.O. Ryu, T.J. Lee, C.H. Chang, J. Electrochem. Synthesis of various zinc oxide nanostructures with zinc acetate Soc. 153 (2006) C382.

[12] T.W. Clyne, P.J. Withers, An Introduction to Metal Matrix Composites, Cambridge, UK, 1995.

[13] T. Graziani, A. Bellosi, D.D. Fabbriche, Int. J. Refract.Fabrication of Al–Zn/α-Al2O3 nanocomposite by mechanical alloying, Met. Hard Mater. 11 (1992) 105–112

[14] K. Konopka, M. Szafran, J. Mater. Process. Bulk Al–Zn/Al2O3 nanocomposite prepared by reactive milling Technol. 175 (2006) 266–270.

[15] Y. Yang, J. Lan, X. Li, Mater. Sci. Eng. A380 (2004) 378–383.

[16] J. Lan, Y. Yang, X. Li, Mater. Sci. Eng. A386 (2004) 284–290.

[17] C. Suryanarayana, Prog. Mater. Sci. 46 (2001) 1–184.

[18] D.G. Kim, J. Kaneko, M. Sugamata, Mater. Trans. 36 (1995) 305–311.

[19] G. Fu, L. Jiang, J. Liu, Y. Wang, J. Univ. Sci. Technol. Beijing 13 (2006) 263–267.

[20] S.C. Tjong, Z.Y. Ma, Mater. Sci. Eng. R: Rep. 29 (2000) 49–113.

[21] G. Chen, G.X. Sun, Z.G. Zhu, Mater. Sci. Eng., A 265 (1999) 197.

[22] G. Chen, G.X. Sun, Mater. Sci. Eng., A 244 (1998) 291.

[23] http://www.chemistry.ohio-state.edu/~woodward/ch754/struct/ZnO.htm

[24] Wang, Zhong Lin, Zinc oxide nanostructures: Growth, properties and applications, J. Phys.: Condens. Matter. Vol. 16 (2004), pp. R829–R858.

[25] Zhong Lin Wang, Nanostructures of ZnO, Materials Today. Vol. 7 (2004) (6), pp. 26-33.

[26] S. Music´, S. Popovic´, M. Maljkovic´, D. Dragcˇevic, Influence of synthesis procedure on the formation and properties of Zinc oxide. Journal of Alloys and Compounds. Vol. 347 (2002), pp. 324–332.

[27] T. K. Subramanyam, B. Srinivasulu Naidu, S. Uthanna, Structure and Optical Properties of DC Reactive Magnetron Sputtered Zinc Oxide Films. Cryst. Res. Technol. Vol. 34 (1999), pp. 981–988.

[28] M. Tavoosi, F. Karimzadeh, M.H. Enayati, A. Heidarpour, Bulk Al–Zn/Al2O3 nanocomposite prepared by reactive milling and hot pressing methodsJournal of Alloys and Compounds 475 (2009) 198–201.

[29] S Baruah and J Dutta, Hydrothermal growth of ZnO nanostructures, Sci. Technol. Adv. Mater. Vol. 10 (2009) (1).

[30] Chen, Z., Z. Shan, S. Li, C.B. Liang, and S.X. Mao. 2004. A novel and simple growth route towards ultra-fine ZnO nanowires. J. Cryst. Growth. Vol. 265, pp. 482–486.

[31] Zhong Lin Wang, Zinc oxide nanostructures: growth, properties and applications, Journal of Physics: Condensed Matter. Vol. 16 (2004), R829- R858.

[32] T. K. Subramanyam, B. Srinivasulu Naidu, S. Uthanna, Physical Properties of Zinc Oxide Films Prepared by dc Reactive Magnetron Sputtering at Different Sputtering Pressures, Cryst. Res. Technol. Vol. 35 (2000), pp. 1193–1202.

[33] Scanning Electron Microscopy (SEM), Susan Swapp, University of Wyoming, Retrieved April 22 2010 from
http://serc.carleton.edu/research_education/geochemsheets/techniques/SEM.html

[34] Energy Dispersive X-ray Spectroscopy (EDS), John Goodge, University of Minnesota-Duluth, Retrieved April 22, 2010 from
http://serc.carleton.edu/research_education/geochemsheets/eds.html

[35] Nicolas Reuge, Revathi Bacs, Chemical Vapor Synthesis of Zinc Oxide Nanoparticles: Experimental and Preliminary Modeling Studies, *J. Phys. Chem. C*, 2009, 113 (46), pp 19845–19852.

[36] Wunderlich, B. (1990). Thermal Analysis. New York: Academic Press. pp. 137–140.

[37] Single Crystal X-ray Diffraction, Christine M. Clark, Eastern Michigan University,Barbara L.Dutrow, Louisiana State University, Retrieved April 22 2010 from
http://serc.carleton.edu/research_education/geochemsheets/techniques/SXD.html

[38]] P. Yang, H. Yan, S. Mao, R. Russo, J. Johnson, R. Saykally, N. Morris, J. Pham, R. He, H.J.Choi, ZnO Nanoribbon microcavity Laser, Adv. Funct. Mater. 12 (2002) 323.

[39]S.Y. Han, D.H. Lee, Y. J. Chang, S. O. Ryu, T. J. Lee, C. H. Chang, Synthesis of various zinc oxide nanostructures with zinc acetate and activated carbon by a matrix-assisted method J. Electrochem. Soc. 153 (2006) C382.

[40] Wu, D., Bai, Z. and Jiang, K., Zinc Oxide Nanostructures Synthesized by Oxidization of ZincMaterials Letters Vol. 63 (2009), pp. 1057–1060.

[41] Huang, M.H., Mao, S., Feick, H., Yan, H. Q, Wu, Y. Y., Kind, H., Preparation of well-aligned ZnO whiskers on glass substrate by atmospheric MOCVD Science Vol. 292 (2001), pp. 1897–99.

[42] Greene,L. E., Law, M., Tan, D. H., Montano, M., GoldbergerJ., Somorjai, G., General Route to Vertical ZnO Nanowire Arrays Using Textured ZnO Seeds Nano Lett. Vol. 5 (2005), pp.1231–6.

[43] C. Suryanarayana, Prog. Synthesis of TiC Powder by Mechanical Alloying of TitaniumMater. Sci. 46 (2001) pp.1–184.

[44] http://en.wikipedia.org.